Active Sites in Sn-β

DOI: 10.1002/anie.201403905

NMR Signatures of the Active Sites in Sn-β Zeolite**

Patrick Wolf, Maxence Valla, Aaron J. Rossini, Aleix Comas-Vives, Francisco Núñez-Zarur, Bernard Malaman, Anne Lesage, Lyndon Emsley, Christophe Copéret, and Ive Hermans**

Abstract: *Dynamic nuclear polarization surface enhanced NMR (DNP-SENS), Mössbauer spectroscopy, and computational chemistry were combined to obtain structural information on the active-site speciation in Sn-β zeolite. This approach unambiguously shows the presence of framework Sn^{IV}-active sites in an octahedral environment, which probably correspond to so-called open and closed sites, respectively (namely, tin bound to three or four siloxy groups of the zeolite framework).*

Heterogeneous catalysts with well-defined isolated active sites do not only facilitate mechanistic investigations, but can also show unparalleled activity in a variety of important reactions. One example is TS-1 for the epoxidation of propene with H_2O_2.[1] A more recent example is Sn-β, which consists of Sn^{IV}-sites embedded in the zeolite-β framework.[2] The uniform distribution of isolated Lewis acid sites, in combination with the unique hydrophobic pore architecture of the material, results in an unrivalled catalytic performance. Of particular interest is the Lewis acid-catalyzed isomerization and epimerization of sugars, key transformations in the upgrading of cellulose-based renewable feedstocks.[3] Sn-β is also active for other reactions, including the Baeyer–Villiger oxidation of ketones and aldehydes,[4] the carbonylene cyclization of citronellal,[5] and the Meerwein—Ponndorf—Verley–Oppenauer reaction.[6] Today, Sn-β can be conveniently synthesized with Sn-loadings varying between 0 and 10 wt %.[7]

[*] P. Wolf,[+] M. Valla,[+] Dr. A. Comas-Vives,[+] Dr. F. Núñez-Zarur,[+] Prof. Dr. C. Copéret
Department of Chemistry and Applied Biosciences, ETH Zurich
Vladimir Prelog Weg 2, 8093 Zurich (Switzerland)
E-mail: ccoperet@ethz.ch

P. Wolf,[+] Prof. Dr. I. Hermans
Department of Chemistry & Department of Chemical and Biological Engineering, University of Wisconsin - Madison
1101 University Avenue, Madison, WI 53706 (USA)
E-mail: hermans@chem.wisc.edu

Dr. A. J. Rossini,[+] Dr. A. Lesage, Prof. Dr. L. Emsley
Centre de RMN à Très Hauts Champs, Institut de Sciences Analytiques, Université de Lyon (CNRS/ENS Lyon/UCB Lyon 1)
69100 Villeurbanne (France)

Prof. Dr. B. Malaman
Institut Jean Lamour-CNRS-UMR 7198, Université de Lorraine, Faculté des Sciences
BP 70239, 54506 Vandoeuvre-les-Nancy (France)

[+] These authors contributed equally to this work.

[**] We acknowledge SNF Grants No. 200021_143600 and 200021_146661, Ambizione project PZ00P2_148059, EQUIPEX contract ANR-10-EQPX-47-01, and ERC Advanced Grant No. 320860 for funding.

Supporting information for this article is available on the WWW under http://dx.doi.org/10.1002/anie.201403905.

Despite the potential of this catalyst, the nature of its active site (distribution) is not fully determined. Various experimental investigations, including the adsorption of deuterated acetonitrile, point towards the presence of several different sites in the material, proposed as closed and open Sn^{IV}-sites, having three and four Sn-O-Si linkages with the zeolite framework, respectively.[8] X-ray absorption fine structure (XAFS) spectroscopy on a 1.6 wt % sample[9] showed that Sn was located in the six-membered ring of the β-framework. The preferred location of Sn^{IV} within the framework (so-called T-sites) is however still the topic of intense experimental and theoretical research.[10] Another open question is how the Sn-loading and -distribution would affect the ratio between closed and opened Sn^{IV}-sites, and which of those sites would be active.

In principle, ^{119}Sn solid-state NMR is an ideal method to probe the local structure at the Sn^{IV} sites. Indeed, major spectral differences have been observed between hydrated and de-hydrated samples, in particular when using isotopically enriched ^{119}Sn (as a result of the low Sn loading, typically a low signal-to-noise ratio is obtained, necessitating ^{119}Sn isotopic labeling).[11] For hydrated samples, the signals observed between $\delta = -685$ and -736 ppm were assigned to octahedral Sn^{IV}. Dehydrated samples are characterized by signals at much higher chemical shift (between $\delta = -425$ and -445 ppm), which have been proposed to correspond to tetrahedral open and closed Sn^{IV} sites, respectively.[12] However, the precise structure of the active sites remains unknown.

Herein we report the determination of the structure of the active sites in Sn-β as a function of Sn loading, by combining Mössbauer, dynamic nuclear polarization surface-enhanced NMR spectroscopy (DNP-SENS) and DFT calculations. Sn-β zeolites with a Sn loading ranging from 0.5–10 wt % were prepared by a two-step post-synthetic method.[7a,b] The synthesized materials were tested for the isomerization of glucose-to-fructose in water, and showed a decreasing turnover frequency (TOF) with increasing Sn loading (Table 1), similar to what has been observed by Sels et al.[7c] This observation suggests the presence of distinct Sn sites with different activities.

No major difference is observed between samples of various loadings in ^{119}Sn Mössbauer spectroscopy, performed at 300 K and 15 K (Figure S1 in the Supporting Information). At 15 K, all spectra show a doublet with the hyperfine parameters, that is, an isomer shift, $IS \approx -0.07(3)$ mm s^{-1} and a quadrupole splitting, $QS \approx 0.75(3)$ mm s^{-1} (Table S1). The observed IS is consistent with a hexacoordinated Sn^{IV} site, with the large QS suggesting a distorted geometry.[13] Moreover, based on the relative increase in spectral area between 300 K and 15 K, the Sn signals were assigned to framework

Table 1: Catalytic activity of Sn-β with different Sn loadings for glucose isomerization in H_2O.[a]

Entry	Catalyst	Sn loading [wt%]	TOF_{init}[b,c] [h^{-1}]
1	Sn-β	0.5	76±15
2	Sn-β	1	64±11
3	Sn-β	2	34±3
4	Sn-β	5	22±0.6
5	Sn-β	10	10±0.2
6	deAl-β	–	N/A[d]
7	SnO_2/deAl-β	10	N/A[d]

[a] Reaction conditions: 100 mg of catalyst in 10 mL of a 5 wt% aqueous glucose solution at 373 K. [b] Defined as the mole product generated per mole Sn per hour calculated at the initial stage of the reaction. [c] Error estimated based on ICP-determined Sn-loading. [d] no product detected by HPLC after 4 h of reaction.

sites. The small asymmetry in the experimental spectra may be due to either texture effects or the presence of minor (less than 2%) additional Sn^{IV} sites. Note that no SnO_2 was detected, consistent with Diffuse Reflectance UV/Vis and Raman data, while small amounts (less than 4%) of Sn^{II} are present, presumably arising from the initial Sn^{II} precursor used for the synthesis of Sn-β.

For NMR spectroscopy in these systems, isotopic enrichment is usually required. Roy et al. have shown that conventional natural isotopic abundance direct polarization ^{119}Sn solid-state NMR spectra of Sn-β can be acquired, but such experiments required between 14 to 60 h of signal averaging for a single 1D ^{119}Sn NMR spectrum.[14]

In a DNP experiment,[15] the nuclear polarization is enhanced by microwave induced polarization transfer from unpaired electrons to nuclei (usually protons). For DNP-SENS the unpaired electrons are introduced by contacting the material by incipient wetness impregnation with a solution of a nitroxide diradical, specifically bulky 2,6-spirocyclohexyl nitroxide derivatives in tetrachloroethane solutions.[16] In the case of nanoparticulate and mesoporous samples, impregnation brings the radical solution into direct contact with the surface of the material allowing the polarization of the protons near the surface to be highly enhanced by DNP. This enhanced ^{1}H polarization is then transferred to the heteronuclei (e.g., ^{13}C, ^{27}Al, ^{29}Si, ^{119}Sn) at the surface.[17] Some of us recently demonstrated the rapid acquisition of natural abundance ^{119}Sn signals in core–shell ligand-capped Sn/SnO_x nanoparticles using DNP-SENS NMR.[18] In our current work, an analogous methodology is used to investigate the molecular structure of the Sn^{IV}-sites in Sn-β.[19]

Samples for ^{119}Sn DNP-SENS were prepared by impregnating the zeolites with a 16 mM solution of TEKPol[20] in tetrachloroethane. Since the pores of Sn-β are quite small (ca. 7 Å diameter), the TEKPol radical is not able to enter the material and cannot interact with the Sn sites. The pores of the Sn-β will be filled with tetrachloroethane and/or water from ambient moisture. Enhanced ^{1}H polarization will be generated at the surface of the Sn-β particles and then transported into the interior of the particles by ^{1}H spin diffusion along the channels (as has been observed for MOF samples).[21] Since the Sn-β particles are quite small (200–400 nm), high ^{1}H DNP enhancements (greater than 60, corresponding to an acceleration by a factor of 3600 in time) were obtained in all cases, enabling the rapid acquisition of natural abundance ^{119}Sn cross-polarization magic-angle spinning (CPMAS) NMR spectra even for low loading levels (0.5 wt% Sn). By comparison, the ^{119}Sn CP NMR spectra acquired without microwave irradiation, and the same number of scans showed no signal, even for high loaded samples. The total spectrometer time required to obtain all the data in Figure 1 was only 3 h. Acquisition can be further

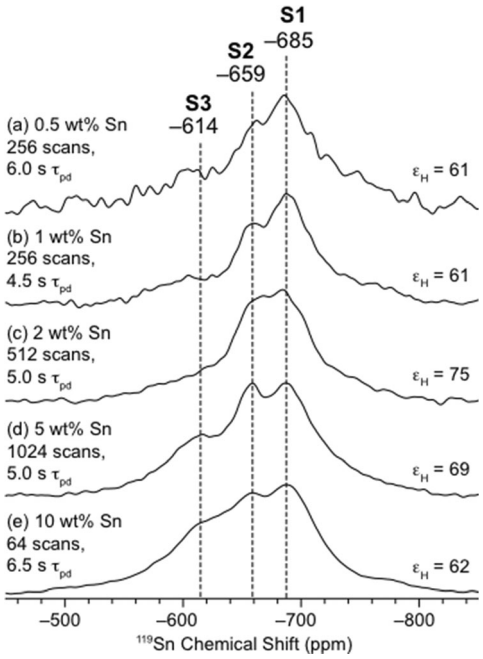

Figure 1. 9.4 T 105 K ^{1}H-^{119}Sn DNP-SENS magic-angle spinning cross-polarization spin echo spectra of a) 0.5 wt% Sn-β zeolite, b) 1 wt% Sn-β zeolite, c) 2 wt% Sn-β zeolite, d) 5 wt% Sn-β zeolite, e) 10 wt% Sn-β zeolite. All samples were impregnated with a 16 mM TEKPol 1,1,2,2-tetrachloroethane solutions. All spectra were acquired with a MAS frequency of 12.5 kHz and CP contact times between 3.0 and 3.5 ms. The number of scans and polarization delay (τ_{pd}) are indicated for each spectrum together with the proton DNP enhancements (ε_H) measured with separate 1H spin echo experiments. The signals around $\delta = -580$ and -780 ppm, as observed for the 10 wt% sample, correspond to spinning sidebands. See text for details.

accelerated by the application of CP-CPMG pulse sequences (Figure S2).[22]

In all spectra, three isotropic Sn chemical shifts centered at approximately $\delta = -614$ (**S3**), -659 (**S2**), and -685 ppm (**S1**) were identified from both 1D CP spin echo (Figure 1) and 2D CPMAT ^{119}Sn spectra (see below). The relative intensity of these sites varies as a function of Sn-loading level (Figure 1 and Figure S3).

Cross-polarization magic-angle turning (CPMAT) experiments[23] were recorded on the 5 and 1 wt% Sn-β samples. A CPMAT spectrum correlates the MAS sideband manifolds to a single isotropic chemical shift in the indirect dimension. This method allows the chemical shift anisotropy (CSA) to be measured for each ^{119}Sn site of the overlapping sideband

manifolds. The Sn CSA arises from the anisotropy of the electronic distribution around the Sn nucleus.

CSA parameters are often described by the isotropic chemical shift (δ_{iso}), the span (Ω) and the skew ($-1 \le \kappa \le +1$) which are calculated from the principal tensor components of the chemical shift tensor $\delta_{11} \ge \delta_{22} \ge \delta_{33}$:[24] [Eq. (1)–(3)].

$$\delta_{iso} = (\delta_{11} + \delta_{22} + \delta_{33})/3 \quad (1)$$

$$\Omega = (\delta_{11} - \delta_{33}) \quad (2)$$

$$\kappa = 3(\delta_{22} - \delta_{iso})/\Omega \quad (3)$$

δ_{iso} is the average of the three components of the CSA tensor and is analogous to the chemical shift that is observed in solution NMR spectroscopy. Ω describes the magnitude of the anisotropy and reports on the degree of spherical symmetry of the electronic distribution at the nuclear site, while κ describes the axial symmetry of the tensor.

The 2D-CPMAT of the 5 wt% Sn-β is shown in Figure 2, where the isotropic NMR spectrum can be observed in the indirect dimension (F_1) and the normal CP spectrum (isotropic peaks and spinning sidebands) can be observed in the direct dimension (F_2). Fitting of the sideband manifolds extracted from the direct dimension at the position of the corresponding provides the CS tensor parameters (δ_{iso}, Ω and κ). The signal **S3** at $\delta = -614$ ppm is similar to that observed for bulk SnO_2, and this site is found to have a Ω of 162 ppm and a κ of $+0.13$, consistent with the octahedral environment of Sn in SnO_2. This resonance has previously been assigned to extra-framework SnO_2 and is typically observed at high Sn-loadings (greater than 1 wt%). In addition, the two other signals at $\delta = -659$ (**S2**) and $\delta = -685$ ppm (**S1**) are associated with slightly different CSA parameters (**S2**: $\Omega = 155$ ppm and $\kappa = +0.05$ and **S1**: $\Omega = 146$ ppm and $\kappa = +0.21$). The chemical shifts and the skews (κ) close to 0 point toward a slightly distorted octahedral Sn environments (see below). The 2D-CPMAT experiment on 1 wt% Sn-β (Figure S4) shows the two peaks at $\delta = -659$ ppm and $\delta = -685$ ppm with similar CSA parameters as observed in the 5 wt% Sn-β sample, consistent with the presence of similar species, suggesting that increased loading does not change the nature of Sn species, but only their ratio.

The one-dimensional ^{119}Sn DNP-SENS CPMAS spectra were deconvoluted (Figure S5) and the relative ratio of each species evaluated (Table 2). Note that since DNP and CP are used to obtain the spectra, it is not possible to quantitatively evaluate the amount of each site, but that this analysis should provide an estimate of the variation of the relative ratio of each site. At low loading, Sn-β is constituted mainly of **S1**, and increased loading leads to increased intensity of **S3**, associated with extra framework SnO_2, while the relative amount of **S2** is approximately constant as a function of the loading level. Reconciling these deconvoluted spectroscopic data with the catalytic activity results in Table 1 suggests that the sites associated with signals **S1** and **S2** are both active in the glucose-to-fructose isomerization (see Figure S6). Note that a significant amount of SnO_2 is detected by DNP-SENS even though it was not observed with Mössbauer, Raman and UV/Vis spectroscopies. It is therefore likely that the SnO_2 clusters are located outside the zeolite framework, closer to the polarizing agent where the DNP enhancement will be higher.

To relate these observations directly to the local structure of the Sn environment, DFT calculations on cluster models were carried out to assign the observed NMR signatures. We first used a small cluster model of the T-site to screen several

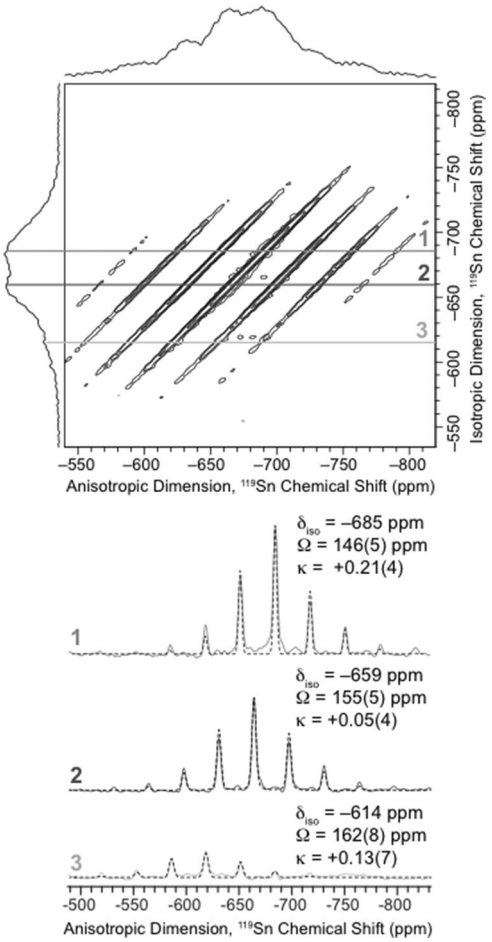

Figure 2. Top: 105 K ^{119}Sn DNP-SENS CP magic-angle turning (CP-MAT) spectra of 5 wt% Sn-β zeolite impregnated with a 16 mM solution of TEKPol in tetrachloroethane. The spectrum was acquired on a 400 MHz DNP spectrometer, with a sample spinning frequency of 5 kHz and a polarization delay of 5 s. 512 scans per increment and 160 t_1 increments were acquired. A ^{1}H DNP enhancement of approximately 85 was obtained. Bottom: Spinning sideband manifolds are shown (1–3) for the three different isotropic shifts and the extracted CS tensor parameters are indicated. Fits of the sideband manifolds are also shown (dashed black lines).

Table 2: Relative contribution of the three ^{119}Sn signals (deconvoluted areas in percentage) as a function of the Snloading as determined from DNP-SENS showing a qualitative trend in active site-distribution.

Entry	Sn loading [wt%]	**S3** [%] $\delta = -614$ ppm	**S2** [%] $\delta = -659$ ppm	**S1** [%] $\delta = -685$ ppm
1	0.5	8	27	65
2	1	8	28	64
3	2	11	36	53
4	5	16	35	49
5	10	24	29	47

structural possibilities and to calibrate the methodology. Details on the models and the methodologies are given in the Supporting Information (see for example, Table S2 for an overview of all structures which were investigated).

For the most realistic cluster model, that includes the zeolite framework, the tetrahedral site has a calculated δ_{iso} of $\delta = -396$ ppm, in good agreement with experimental values (see above), and the chemical shift decreases by approximately 100 ppm with the addition of each (1 or 2) coordinated water molecule (see Supporting Information). The hexacoordinated Sn sites, resulting from the coordination/reaction of at least two water molecules, have calculated NMR parameters consistent with the experimental values. When Sn-sites have two water molecules in the first coordination sphere and one additional water molecule H-bonded to the coordinated H_2O, the calculated NMR parameters are in very good agreement with the experimental chemical shift parameters: $\delta_{iso}/\Omega/\kappa$ of $-654/228/0.31$ and $-684/248/0.02$ for open or closed sites, respectively, allowing the assignment of **S2** ($\delta = -654$ ppm) to an open site and **S1** ($\delta = -685$ ppm) to a closed site, coordinated by two H_2O molecules (Scheme 1).

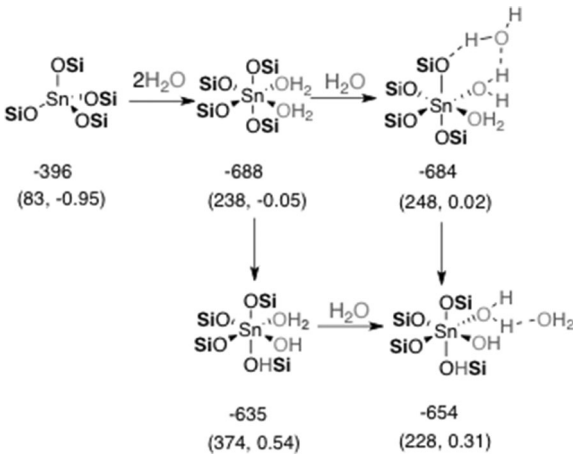

Scheme 1. Computed ^{119}Sn isotropic chemical shifts in ppm (δ_{iso} upper numbers outside of parenthesis). The span Ω (in ppm) and skew κ are shown in parenthesis (see also Supporting Information).

The low Ω and a value of κ close to 0 are consistent with distorted octahedral sites. In terms of stability, the T_1 sites with two coordinated water molecules (closed site) are energetically more favored by approximately 5 kcal mol^{-1} than the corresponding opened site with one coordinated H_2O and one Sn-O-Si bridge opened by H_2O (Table S4). However, the presence of an additional water molecule on the second coordination sphere is crucial to stabilize the opened site structure by hydrogen bonding (see Table S4), which is otherwise highly unstable (+ 19 kcal mol^{-1}).

In summary, combining Mössbauer spectroscopy, DNP-SENS, and DFT calculations show that the active sites of Sn-β zeolite correspond to octahedrally coordinated Sn^{IV}, involving the tetrahedral Sn-sites and two water molecules. In agreement with earlier literature hypotheses two types of Sn are determined herein: one where two water molecules are coordinated to Sn (closed site), and another where one of the water molecules has opened one of the Sn-O-Si bridges (open site). These two species, with distinct NMR signatures, are the active sites of Sn-β zeolite.

Experimental Section

Sn-β samples were synthesized and characterized as described elsewhere.[7a] Glucose isomerization reactions in H_2O were carried out in a 25 mL sealed round bottom flask. The vessel was charged with aqueous glucose solution (10 mL of 5 wt %) and heated to 100 °C for 15 min, prior to the addition of catalyst (100 mg). The reaction mixture was stirred vigorously at 500 rpm for the required reaction period. Samples were taken periodically and quantified by HPLC equipped with an RI detector. Monosaccharides were separated using a Ca^{2+} column (Phenomenex).

^{119}Sn Mössbauer measurements were carried out using a constant-acceleration spectrometer in standard transmission geometry with a $Ba^{119m}SnO_3$ source (10 mCi) kept at room temperature as a reference for the isomer shifts. Spectra of each sample were recorded at 300 and 15 K in a liquid helium cryostat. The velocity scale was calibrated with a ^{57}CoRh source (25 mCi) and a metallic iron foil at room temperature. A polycrystalline absorber with natural abundance of ^{119}Sn isotope and thickness of 15 mg cm^{-2} was used. A palladium foil of 0.5 mm thickness was used as a critical absorber for tin X-rays. The Mössbauer spectra were fitted by using a unique doublet with a FWHM value of around 1.0 mm s^{-1} (see Table S1) with a least-squares method program assuming Lorentzian.[25]

DNP solid-state NMR experiments were performed on a Bruker Avance III 9.4 T (400 MHz/263 GHz ^{1}H/electron Larmor frequencies) DNP spectrometer[26] equipped with a gyrotron microwave source. The sweep coil of the main superconducting NMR coil was set so that microwave irradiation occurred at the positive enhancement maximum for the TOTAPOL diradical.[27] Samples were prepared for DNP-SENS experiments by applying incipient wetness impregnation with a 16 mM solution of the TEKPol[20] biradical in 1,1,2,2-tetrachloroethane to the Sn-β zeolite materials. Typically the material (25 mg) was impregnated with biradical solution (20 μL) then packed into 3.2 mm outer diameter sapphire rotors. The ^{119}Sn spectra were acquired with a rotor synchronized CP spin echo pulse sequence and the full spin echo signal was acquired. CP experiments were typically performed with a 2.5 μs ^{1}H π/2 pulse for excitation and ^{1}H and ^{119}Sn spin lock rf fields of ca. 72 kHz and MAS frequencies of 12.5 kHz. The amplitude of the ^{1}H spin lock pulse was linearly ramped from 90 to 100 % of its maximum value. Optimized contact times of 3.0 to 3.5 ms were used. SPINAL-64 heteronuclear ^{1}H decoupling was applied in all experiments.[27] The constant time five-π pulse MAT experiment of Grant and co-workers was employed for acquisition of the 2D ^{119}Sn chemical shift correlation spectra.[23] CS tensor parameters were obtained by fitting the sideband manifolds with the HBA-Graphic Analysis Program *v*1.7.3 (Dr. K. Eichele, University of Tübingen).

Received: April 1, 2014
Revised: May 28, 2014
Published online: July 30, 2014

Keywords: active sites · DNP SENS · Mössbauer spectroscopy · solid-state NMR spectroscopy · zeolites

[1] a) F. Cavani, J. H. Teles, *ChemSusChem* **2009**, *2*, 508 – 534; b) B. Notari, *Adv. Catal.* **1996**, *41*, 253 – 334; c) S. Bordiga, A. Damin, F. Bonino, C. Lamberti, *Surface and Interfacial Organometallic Chemistry and Catalysis*, *Vol. 16* (Eds.: C. Copéret, B. Chaudret), Springer, Berlin, **2005**, pp. 37 – 68.

[2] a) Y. Román-Leshkov, M. Davis, *ACS Catal.* **2011**, *1*, 1566 – 1580; b) R. Lobo, *AIChE J.* **2008**, *54*, 1402 – 1409; c) M. Dusselier, P. Van Wouwe, A. Dewaele, E. Makshina, B. F. Sels, *Energy Environ. Sci.* **2013**, *6*, 1415 – 1442.

[3] a) M. S. Holm, S. Saravanamurugan, E. Taarning, *Science* **2010**, *328*, 602 – 603; b) Y. Román-Leshkov, M. Moliner, J. A. Labinger, M. E. Davis, *Angew. Chem.* **2010**, *122*, 9138 – 9141; *Angew. Chem. Int. Ed.* **2010**, *49*, 8954 – 8957; c) M. Moliner, Y. Román-Leshkov, M. E. Davis, *Proc. Natl. Acad. Sci. USA* **2010**, *107*, 6164 – 6168; d) W. R. Gunther, Y. Wang, Y. Ji, V. K. Michaelis, S. T. Hunt, R. G. Griffin, Y. Román-Leshkov, *Nat. Commun.* **2012**, *3*, 1109 – 1116.

[4] a) A. Corma, L. Nemeth, M. Renz, S. Valencia, *Nature* **2001**, *412*, 423 – 425; b) A. Corma, V. Fornés, S. Iborra, M. Mifsud, M. Renz, *J. Catal.* **2004**, *221*, 67 – 76; c) M. Renz, T. Blasco, A. Corma, V. Fornés, R. Jensen, L. Nemeth, *Chem. Eur. J.* **2002**, *8*, 4708 – 4717.

[5] A. Corma, M. Renz, *Chem. Commun.* **2004**, 550 – 551.

[6] a) A. Corma, M. E. Domine, L. Nemeth, S. Valencia, *J. Am. Chem. Soc.* **2002**, *124*, 3194 – 3195; b) M. Boronat, A. Corma, M. Renz, *J. Phys. Chem. B* **2006**, *110*, 21168 – 21174; c) A. Corma, M. E. Domine, S. Valencia, *J. Catal.* **2003**, *215*, 294 – 304.

[7] a) C. Hammond, S. Conrad, I. Hermans, *Angew. Chem.* **2012**, *124*, 11906 – 11909; *Angew. Chem. Int. Ed.* **2012**, *51*, 11736 – 11739; b) P. Wolf, C. Hammond, S. Conrad, I. Hermans, *Dalton Trans.* **2014**, *43*, 4514 – 4519; c) J. Dijkmans, D. Gabriëls, M. Dusselier, F. de Clippel, P. Vanelderen, K. Houthoofd, A. Malfliet, Y. Pontikes, B. F. Sels, *Green Chem.* **2013**, *15*, 2777 – 2785; d) P. Li, G. Liu, H. Wu, Y. Liu, J. Jiang, P. Wu, *J. Phys. Chem. C* **2011**, *115*, 3663 – 3670.

[8] a) M. Boronat, P. Concepción, A. Corma, M. Renz, S. Valencia, *J. Catal.* **2005**, *234*, 111 – 118; b) M. Boronat, P. Concepción, A. Corma, M. Renz, *Catal. Today* **2007**, *121*, 39 – 44.

[9] S. R. Bare, S. D. Kelly, W. Sinkler, J. J. Low, F. S. Modica, S. Valencia, A. Corma, L. T. Nemeth, *J. Am. Chem. Soc.* **2005**, *127*, 12924 – 12932.

[10] a) G. Yang, E. Pidko, E. J. M. Hensen, *J. Phys. Chem. C* **2013**, *117*, 3976 – 3986; b) G. Yang, E. A. Pidko, E. J. M. Hensen, *ChemSusChem* **2013**, *6*, 1688 – 1696.

[11] R. Bermejo-Deval, R. S. Assary, E. Nikolla, M. Moliner, Y. Román-Leshkov, S.-J. Hwang, A. Palsdottir, D. Silverman, R. F. Lobo, L. A. Curtiss, M. E. Davis, *Proc. Natl. Acad. Sci. USA* **2012**, *109*, 9727 – 9732.

[12] R. Bermejo-Deval, R. Gounder, M. E. Davis, *ACS Catal.* **2012**, *2*, 2705 – 2713.

[13] Tetrahedral Sn^{IV} is expected with significant negative value (IS = $-0.2\ mm\,s^{-1}$), corroborating the hexacoordination of Sn in the sample; R. V. Parish in *Mossbauer Spectroscopy Applied to Inorganic Chemistry*, *Vol. 1* (Ed.: G. J. Long) Plenum, New York, **1984**, p. 527.

[14] S. Roy, K. Bakhmutsky, E. Mahmoud, R. F. Lobo, R. J. Gorte, *ACS Catal.* **2013**, *3*, 573 – 580.

[15] T. Maly, G. T. Debelouchina, V. S. Bajaj, K. N. Hu, C. G. Joo, M. L. Mak-Jurkauskas, J. R. Sirigiri, P. C. A. van der Wel, J. Herzfeld, R. J. Temkin, R. G. Griffin, *J. Chem. Phys.* **2008**, *128*, 052211.

[16] a) A. Zagdoun, A. J. Rossini, D. Gajan, A. Bourdolle, O. Ouari, M. Rosay, W. E. Maas, P. Tordo, M. Lelli, L. Emsley, A. Lesage, C. Copéret, *Chem. Commun.* **2012**, *48*, 654 – 656; b) A. Zagdoun, G. Casano, O. Ouari, G. Lapadula, A. Rossini, M. Lelli, M. Baffert, D. Gajan, L. Veyre, W. Maas, M. Rosay, R. Weber, C. Thieuleux, C. Coperet, A. Lesage, P. Tordo, L. Emsley, *J. Am. Chem. Soc.* **2012**, *134*, 2284 – 2291; c) D. Gajan, M. Schwarzwälder, M. P. Conley, W. R. Gruening, A. J. Rossini, A. Zagdoun, M. Lelli, M. Yulikov, G. Jeschke, C. Sauvée, O. Ouari, P. Tordo, L. Veyre, A. Lesage, C. Thieuleux, L. Emsley, C. Copéret, *J. Am. Chem. Soc.* **2013**, *135*, 15459 – 15466.

[17] a) A. Lesage, M. Lelli, D. Gajan, M. A. Caporini, V. Vitzthum, P. Miéville, J. Alauzun, A. Roussey, C. Thieuleux, A. Mehdi, G. Bodenhausen, C. Copéret, L. Emsley, *J. Am. Chem. Soc.* **2010**, *132*, 15459 – 15461; b) M. Lelli, D. Gajan, A. Lesage, M. A. Caporini, V. Vitzthum, P. Miéville, F. Héroguel, F. Rascon, A. Roussey, C. Thieuleux, M. Boualleg, L. Veyre, G. Bodenhausen, C. Copéret, L. Emsley, *J. Am. Chem. Soc.* **2011**, *133*, 2104 – 2107; c) A. Rossini, A. Zagdoun, M. Lelli, A. Lesage, C. Copéret, L. Emsley, *Acc. Chem. Res.* **2013**, *46*, 1942 – 1951.

[18] L. Protesescu, A. J. Rossini, D. Kriegner, M. Valla, A. de Kergommeaux, M. Walter, K. V. Kravchyk, M. Nachtegaal, J. Stangl, B. Malaman, P. Reiss, A. Lesage, L. Emsley, C. C. Copéret, M. V. Kovalenko, *ACS Nano* **2014**, *8*, 2639 – 2648.

[19] After submission of this manuscript the following paper appeared on the use of DNP enhanced ^{119}Sn NMR for hydrothermally synthesized Snβ: W. R. Gunther, V. K. Michaelis, M. A. Caporini, R. G. Griffin, Y. Román-Leshkov, *J. Am. Chem. Soc.* **2014**, *136*, 6219 – 6222.

[20] A. Zagdoun, G. Casano, O. Ouari, M. Schwarzwälder, A. J. Rossini, F. Aussenac, M. Yulikov, G. Jeschke, C. Copéret, A. Lesage, P. Tordo, L. Emsley, *J. Am. Chem. Soc.* **2013**, *135*, 12790 – 12797.

[21] a) P. C. A. van der Wel, K. N. Hu, J. Lewandowski, R. G. Griffin, *J. Am. Chem. Soc.* **2006**, *128*, 10840 – 10846; b) A. J. Rossini, A. Zagdoun, F. S. Hegner, M. Schwarzwälder, D. Gajan, C. Copéret, A. Lesage, L. Emsley, *J. Am. Chem. Soc.* **2012**, *134*, 16899 – 16908; c) O. Lafon, A. S. L. Thankamony, T. Kobayashi, D. Carnevale, V. Vitzthum, I. Slowing, K. Kandel, H. Vezin, J. P. Amoureux, G. Bodenhausen, M. Pruski, *J. Phys. Chem. C* **2013**, *117*, 1375 – 1382; d) A. J. Rossini, A. Zagdoun, M. Lelli, J. Canivet, S. Aguado, O. Ouari, M. Rosay, W. E. Maas, C. Copéret, D. Farrusseng, L. Emsley, A. Lesage, *Angew. Chem.* **2012**, *124*, 127 – 131; *Angew. Chem. Int. Ed.* **2012**, *51*, 123 – 127.

[22] A. J. Rossini, A. Zagdoun, M. Lelli, D. Gajan, F. Rascón, M. Rosay, W. E. Maas, C. Copéret, A. Lesage, L. Emsley, *Chem. Sci.* **2012**, *3*, 108 – 115.

[23] J. Z. Hu, W. Wang, F. Liu, M. S. Solum, D. W. Alderman, R. J. Pugmire, D. M. Grant, *J. Magn. Reson. Ser. A* **1995**, *113*, 210 – 222.

[24] J. Herzfeld, A. E. Berger, *J. Chem. Phys.* **1980**, *73*, 6021.

[25] G. Le Caër, personal communication.

[26] M. Rosay, L. Tometich, S. Pawsey, R. Bader, R. Schauwecker, M. Blank, P. M. Borchard, S. R. Cauffman, K. L. Felch, R. T. Weber, R. J. Temkin, R. G. Griffin, W. E. Maas, *Phys. Chem. Chem. Phys.* **2010**, *12*, 5850 – 5860.

[27] B. M. Fung, A. K. Khitrin, K. J. Ermolaev, *J. Magn. Reson.* **2000**, *142*, 97 – 101.

